Geomechanics and Engineering, *Vol. 11, No. 3 (2016) 373-383*
DOI: http://dx.doi.org/10.12989/gae.2016.11.3.373

Fracture of rock affected by chemical erosion environment

W. Gao* and M.M. Ge [a]

Key Laboratory of Ministry of Education for Geomechanics and Embankment Engineering, College of Civil and Transportation Engineering, Hohai University, Nanjing 210098, P.R. China

(*Received April 12, 2015, Revised March 09, 2016, Accepted May 11, 2016*)

Abstract. As one natural material, the physical and mechanical properties of rock will be affected very largely by chemical erosion environment. Under chemical environment, the strength of rock will be reduced. Considering the effect of the chemical erosion, fracture factor of rock is reduced. The damage variable is applied to express the change of fracture stress. Therefore, the fracture criterion of rock under chemical environment is constructed. By one experiment of rock fracture under chemical erosion environment, the proposed fracture criterion is verified. The results show that, the fracture path by theory is agree with the testing one well.

Keywords: chemical erosion; environment effect; fracture; rock; crack

1. Introduction

Rock is one discontinuous, heterogeneous and anisotropic geological body. The expanding and communicating of the discontinuities, such as joint and fissure, are the key cause of the rock broken. Therefore, the theory and experiment studies on the principles of fissure expanding and communicating are the main problem of rock mechanics (Gao *et al*. 2015, Liu *et al*. 2014, Pu and Cao 2012, Wei *et al*. 2015, Yu *et al*. 2014, Zhang *et al*. 2010).

As one natural geological body, rock is generally corroded by the water-chemical environment, such as the acid rain, pollution water, etc. (Mukhopadhyay *et al*. 2013, Grgic and Giraud 2014, Guo *et al*. 2014). For the erosion, the connection of mineral particles in the rock is weakened, and the physical and mechanical properties of rock are deviated for the change of granular lattice. At the same time, the water chemical solution can corrode the rock and carry out the dissolution materials. Therefore, the property of rock will become bad, and then the rock engineering will be dangerous. Because it is very important to study on the affection of the chemical erosion to the rock material, nowadays, there are some researches on this field (Chen *et al*. 2014, Ding and Feng 2009, Feng *et al*. 2010, Kazempour 2012, Li *et al*. 2014, Min *et al*. 2009, Pandey *et al*. 2014, Poulet *et al*. 2012, Taron *et al*. 2009, Wang 2012, Zhao *et al*. 2014). For it is a new research field of rock mechanics, it still requires some improvements.

In this study, based on the energy fracture criterion proposed by author, the new fracture criterion for rock with multi-preexisting cracks under chemical erosion is proposed. At last, based on the experiment of rock fracture under chemical erosion, the proposed fracture criterion is

*Corresponding author, Professor, E-mail: wgaowh@163.com
[a] Master, E-mail: 775326695@qq.com

http://www.techno-press.org/?journal=gae&subpage=7 ISSN: 2005-307X (Print), 2092-6219 (Online)

verified.

2. Fracture principles for rock with cracks under chemical erosion

From previous studies (Feng *et al*. 2010), the erosion affect of the chemical solution on the rock is reflected by the change of elastic modulus. However, considering the cracks in the rock, it is reflected by the increase of crack length and the decrease of fracture stress. Therefore, the fracture factor of rock is reduced, and the damage variable is applied to express the change of fracture stress. Then, the fracture criterion of rock with cracks under chemical erosion can be constructed.

From previous studies (Gao *et al*. 2011), the fracture criterion of rock with cracks based on the energy principles is as follows

$$\begin{aligned}&(3-4\mu-\cos\theta)(1+\cos\theta)K_I^2+4\sin\theta(2\mu-1+\cos\theta)K_I K_{II}\\&+[4(1-\mu)(1-\cos\theta)+(1+\cos\theta)(3\cos\theta-1)]K_{II}^2=4(1-2\mu)K_{Ic}^2\end{aligned} \tag{1}$$

where, K_I, K_{Ic} are the stress intensity factor and the fracture toughness of crack mode I,
K_{II} is the stress intensity factor of crack mode II,
θ is the angular coordinate,
μ is the Poisson ratio.

The model for the rock crack is as shown in Fig. 1.

According to the theories of the fracture mechanics (Gross and Seelig 2011), the normal stress and shear stress on the surface of crack are as follows

$$\sigma=\frac{1}{2}[(\sigma_1+\sigma_3)-(\sigma_1-\sigma_3)\cos 2\beta] \tag{2}$$

$$\tau=\frac{1}{2}\{(\sigma_1-\sigma_2)\sin 2\beta-\mu[(\sigma_1+\sigma_2)+(\sigma_1-\sigma_2)\cos 2\beta]\} \tag{3}$$

Without chemical erosion, based on the linear elastic fracture mechanics (Gross and Seelig2011), there are follows equations

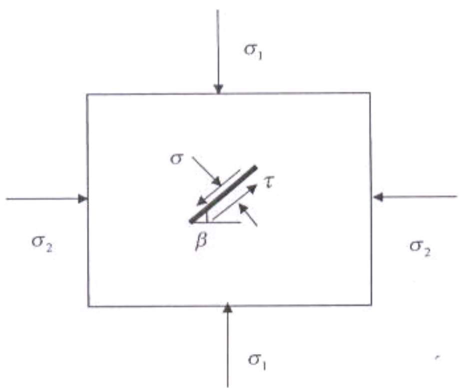

Fig. 1 Simple model for rock crack

$$K_I = \sigma\sqrt{\pi a}\ , \quad K_{Ic} = \sigma_c\sqrt{\pi a} \tag{4}$$

$$K_{II} = \tau\sqrt{\pi a}\ , \quad K_{IIc} = \tau_c\sqrt{\pi a} \tag{5}$$

where, K_{IIc} is the fracture toughness of crack mode II,
a is the length of crack,
σ_c and τ_c are the fracture stresses of rock.

Therefore, the initial cracking stress intensity factors of crack modes I and II under compression-shear state are as follows

$$K_I = \frac{\sqrt{\pi a}}{2}\left[(\sigma_1+\sigma_2)-(\sigma_1-\sigma_2)\cos 2\beta\right] \tag{6}$$

$$K_{II} = \frac{\sqrt{\pi a}}{2}\left\{(\sigma_1-\sigma_2)\sin 2\beta - \mu\left[(\sigma_1+\sigma_2)+(\sigma_1-\sigma_2)\cos 2\beta\right]\right\} \tag{7}$$

Based on the complex variable function method (Horri and Nemat-Nasser 1985), from the sliding crack model (Horri and Nemat-Nasser 1985, Gross and Seelig 2011), the expanding cracking stress intensity factors are as follows

$$\begin{cases} K_I = \dfrac{2a\tau_{eff}\sin\theta}{\sqrt{\pi(l+l^*)}} - \sigma_n'\sqrt{\pi l} \\ K_{II} = \dfrac{2a\tau_{eff}\sin\theta}{\sqrt{\pi(l+l^*)}} - \tau_n'\sqrt{\pi l} \end{cases} \tag{8}$$

where, l^* is the equivalent expanding crack length to fit the analytical solution, which almost equals to $0.27a$.
l is the length of the main crack,
τ_{eff} is the equivalent shear for the main crack,
σ_n' and τ_n' are the normal stress and shear stress on the surface of the main crack, which can be described as

$$\begin{cases} \sigma_n' = \dfrac{1}{2}\left[(\sigma_1+\sigma_2)+(\sigma_1-\sigma_2)\cos 2(\theta+\beta)\right] \\ \tau_n' = \dfrac{1}{2}\left[(\sigma_1+\sigma_2)\cos 2(\theta+\beta)\right] \end{cases} \tag{9}$$

The detailed descriptions for the above Eq. (8) can be found in reference (Gross and Seelig 2011).

Considering the effect of the chemical erosion, to compute simply, the same damage variable D is applied to the crack length and the fracture stress. Thus, from Eqs. (4) and (5), the stress intensity factors and the fracture toughness of crack modes I and II are as follows

$$K_I = \sigma\sqrt{\pi a(1+D)}\ , \quad K_{Ic} = \sigma_c(1-D)\sqrt{\pi a} \tag{10}$$

$$K_{II} = \tau\sqrt{\pi a(1+D)}\ , \quad K_{IIc} = \tau_c(1-D\ )\sqrt{\pi a} \tag{11}$$

The initial cracking stress intensity factors of crack modes I and II are as follows

$$K_I = \frac{\sqrt{\sigma a(1+D)}}{2}\left[(\sigma_1+\sigma_2)-(\sigma_1-\sigma_2)\cos 2\beta\right] \tag{12}$$

$$K_{II} = \frac{\sqrt{\sigma a(1+D)}}{2}\left\{(\sigma_1-\sigma_2)\sin 2\beta - \mu\left[(\sigma_1+\sigma_2)+(\sigma_1-\sigma_2)\cos 2\beta\right]\right\} \tag{13}$$

The expanding cracking stress intensity factors are as follows

$$\begin{cases} K_I = \dfrac{2a(1+D)\tau_{eff}\sin\theta}{\sqrt{\pi\left(l+l^*\right)}} - \sigma_n{}'\sqrt{\pi l} \\ K_{II} = \dfrac{2(1+D)\tau_{eff}\sin\theta}{\sqrt{\pi\left(l+l^*\right)}} - \tau_n{}'\sqrt{\pi l} \end{cases} \tag{14}$$

When the K_I increases to the critical stress intensity factor, there are follow equation

$$K_I = K_{Ic} \tag{15}$$

From the Eq. (1), there are follow equations

$$\sigma\sqrt{1+D}\sqrt{\pi a}\,/(1-D) = \sigma_c\sqrt{\pi a} \tag{16}$$

$$K_{Ic} = \sigma\sqrt{1+D}\sqrt{\pi a}\,/(1-D) \tag{17}$$

$$K_{IIc} = \tau\sqrt{1+D}\sqrt{\pi a}\,/(1-D) \tag{18}$$

The Eqs. (10)-(13) and (16)-(17) are all substituted the parameters in Eq. (1), and then, the fracture criterion for rock with cracks under chemical erosion can be obtained.

As $K_I = K_{Ic}$, the normal stress for the crack whose expanding length is $2l$ is as follows

$$\sigma_1 = \frac{\sqrt{b\sin(\pi l/b)}\left[K_{Ic}+\sigma_2\sqrt{2b\tan(\pi l/2b)}\right]}{\sin\theta\left[c(\sin 2\theta-\mu\cos 2\theta)-\mu/2\right]} + \frac{\sigma_2\left[c(\sin 2\theta-\mu\cos 2\theta)+\mu/2\right]}{c(\sin 2\theta-\mu\cos 2\theta)-\mu/2} \tag{19}$$

where, b is the space between the cracks,
c is the original length of crack.

At the nearby of the free surface, $\sigma_2 = 0$, therefore, the Eq. (19) can be described as follows

$$\sigma_1 = \frac{\sqrt{b\sin(\pi l/b)}K_{Ic}}{\sin\theta\left[c(\sin 2\theta-\mu\cos 2\theta)-\mu/2\right]} \tag{20}$$

The critical expanding length of crack in the rock is as follows

$$l' = \frac{b}{\pi}\arcsin\left\{\frac{1}{b}\left[\frac{\sigma_1^2 \sin^2\theta\left[c\left(\sin 2\theta - \mu\cos 2\theta\right) - \mu/2\right]^2}{K_{Ic}^2}\right]\right\} \tag{21}$$

When the stress σ_1 increases to the critical value σ_{1c}, the initial cracking will grow at the crack tip. And then, the crack will expand until its length is to the critical expanding length. As the stress increases, the crack expanding condition is satisfied, and then the cracks will expand quickly. Therefore, the cracks will communicate, and the rock will be broken.

3. Experiment verification

3.1 Introduction of the experiment

The specimens are sandstone and limestone. Their mechanics parameters are as follows,

For the sandstone, the Young's modulus E is 2.8×10^4 MPa, the Poisson's ratio μ is 0.25.

For the limestone, the Young's modulus E is 3.5×10^4 MPa, the Poisson's ratio μ is 0.15.

The chemical solution is NaCl solution, whose concentration is 0.01mol/L. The PH values of solution are 2, 7 and 12.

The specimen is one cuboid, whose length, width and height are 50 mm, 50 mm and 100 mm, respectively. Three cracks are executed in the specimen. From top to bottom, the cracks are marked as crack 1, crack 2 and crack 3. The inclination of cracks are as follows, 45°, 45° and 105°. The lengths of the cracks are all 10 mm. The spacing intervals are all 20 mm. The layout of the specimen is shown in Fig. 2.

In each experiment, one group of specimens for sandstone and limestone, respectively, are used. In each group, there are five specimens. The specimens are putted into the chemical solution and soaked for about 28 days. After the specimen was soaked in the solution for the given time, it was tested. In the testing, the specimen is put into the loading box. And the chemical solution is injected into the box. Then the loading box is used for compression test. At last, the damage process curves and acoustic emission process curves can be obtained. Because the testing laws under three PH values are the same, the typical results for PH value of 2 are used in this study.

The typical results of acoustic emission test are shown in Figs. 3 and 4.

As shown in Fig. 3, when the stress reaches to the 20% of the strength, the acoustic emission events in the specimen is little and separate distribution. In this stage, the original cracks and

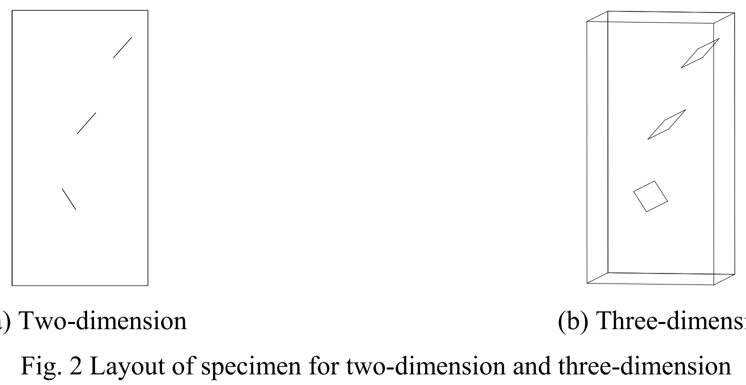

(a) Two-dimension (b) Three-dimension

Fig. 2 Layout of specimen for two-dimension and three-dimension

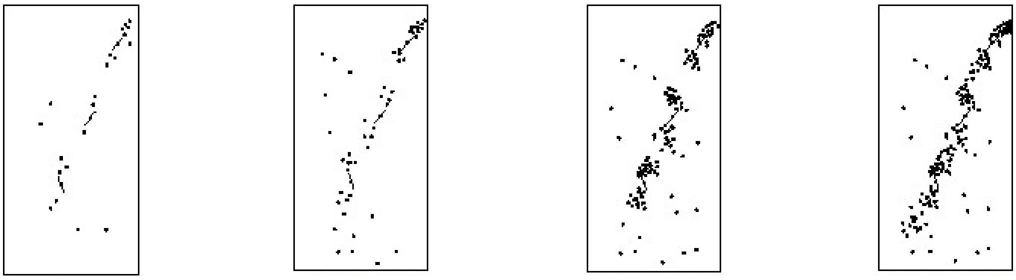

(a) 20%-30% of strength (b) 30%-60% of strength (c) 60%-90% of strength (d) 90%-1000% of strength

Fig. 3 Acoustic emission test results for limestone specimen in the solution whose PH value is 2

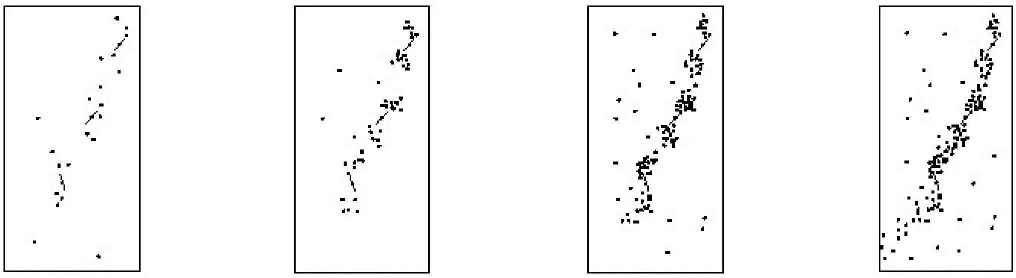

(a) 20%-30% of strength (b) 30%-60% of strength (c) 60%-90% of strength (d) 90%-1000% of strength

Fig. 4 Acoustic emission test results for sandstone specimen in the solution whose PH value is 2

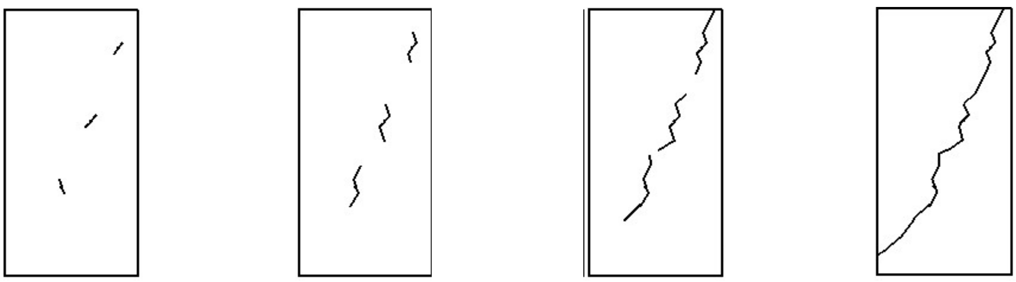

(a) Sandstone

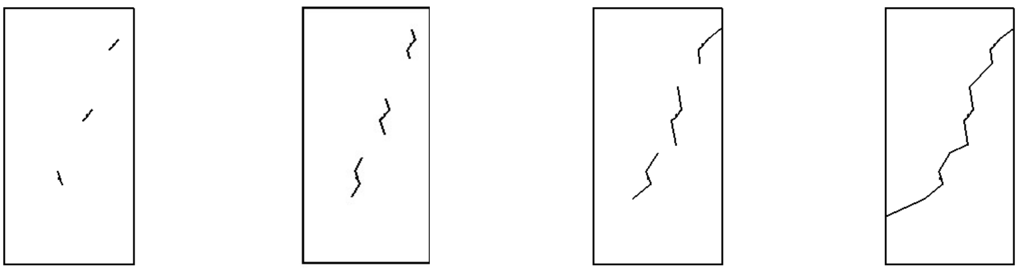

(b) Limestone

Fig. 5 Fracture process of rock specimen in the solution whose PH value is 2 defects will be squeezed. When the stress reaches to the 30-50% of the strength, the original cracks will be extended, and the acoustic emission events will centralize in the range of the crack tip. When the stress reaches to the 60-80% of the strength, the acoustic emission events will be more and more concentrated, and distributes along one path. When the stress reaches to the 100% of the strength, the acoustic emission events distributes very concentration, and the cracks communicate. As shown in Fig. 4, the process of the sandstone specimen is the same with that of the limestone specimen. But the fracture process of sandstone is slow, and the acoustic emission events are less. Therefore, the influence of chemical corrosion on the limestone is more seriously than that on the sandstone.

Based on above test results, the fracture process of rock specimens can be obtained, which are as shown in Fig. 5.

3.2 Theory analysis of the fracture process

Because the spacing interval between the adjacent cracks is large and the volume is small, to simplify the computation, the computing of the stress intensity factor at the crack tip is not affected by other cracks. This hypothesis is only used at the beginning of the crack expanding. In the later period of crack expansion, the spacing interval between the adjacent cracks will be little, therefore, the effect of adjacent cracks must be considered. Thus, the improved Kachanov method (Jaeger *et al*. 2009) is used to analyze the interrelationship of cracks after the crack expanding. In this method, the traction in a crack is decomposed into a linearly varying component and a non-uniform component. The magnitude of each component is computed by assuming the resultant force of the non-uniform component to be zero and the sum of the two components to be equal to the total traction at every point along the crack length. In considering the interaction between the two cracks, the effect of the non-uniform component is ignored. The linearly varying component is chosen in such a way that it is in equilibrium with the pseudotraction. It is further assumed that the interaction effect due to the non-uniform component can be neglected, and therefore, only the effect of the linearly varying component has to be considered. Based on equivalence principle, the pseudotractions of the cracks can be obtained. For each crack, the average tractions equations can be established. Therefore, there will be a number of equations, which equals to the double number of the cracks, with the same number of ‘average’ tractions as the unknowns. On solving these equations, we can determine the ‘average’ tractions. Having the ‘average’ tractions determined, one can then obtain the updated tractions acting on these cracks and determine the stress intensity factors for each crack in the usual manner.

For the sandstone, the fracture toughness of crack modes I and II for three cracks at beginning are all K_{IC} = 0.75 Mpa·m$^{1/2}$ and K_{IIC} = 0.43 Mpa·m$^{1/2}$. The friction coefficient is 0.2.

Because the initial cracks are under compression-shear state, the initial cracking fracture criterion is as follows

$$K_{\mathrm{I}} \sin\theta_c + K_{\mathrm{II}}(3\cos\theta_c - 1) = 0 \tag{22}$$

$$\begin{aligned}&(3-4\mu-\cos\theta)(1+\cos\theta)K_I^2 + 4\sin\theta(2\mu-1+\cos\theta)K_I K_{II}\\&+[4(1-\mu)(1-\cos\theta)+(1+\cos\theta)(3\cos\theta-1)]K_{II}^2 = 4(1-2\mu)K_{Ic}^2\end{aligned} \tag{23}$$

According to previous study (Feng *et al*. 2010), the damage variable D can be described as follows

$$D = -Exp[m_1 + m_2 Exp[pH] + m_3 Exp[-pH]] + 0.8032 \tag{24}$$

where, m_1, m_2 and m_3 are material parameters, which can be determined by the experiment.

The Eq. (24) mainly considers the affection of chemical erosion on the Young's modulus, but under real chemical erosion condition, the void in the rock will grow. To consider the affection of chemical erosion comprehensively, from the general multiple relationships between the main variables and secondary variables, based on the testing results in our study, the above function should be improved. Therefore, one correction factor which is 1.05 is introduced into the Eq. (24). Moreover, the experimental constant also has been corrected. It must be point that the correction factor is one experience value and from the summary of the experimental results. Therefore, the damage variable D can be described as follows

$$D = -1.05 Exp[m_1 + m_2 Exp[pH] + m_3 Exp[-pH]] + 0.8434 \tag{25}$$

For the sandstone specimen which is corroded by the chemical solution whose PH value is 2, the material parameters are as follows, $m_1 = -1.0974$, $m_2 = -1.679811\times10^{-4}$, $m_3 = -2.0493$.

The expanding length of crack can be computed by Eq. (21).

According to Eqs. (21), (22), and (23) the initial cracking angles and initial cracking lengths of all cracks are as follows,

As for crack 1, $\theta_{c1} = 45.22°$, $l_1 = 0.008$ m.
As for crack 2, $\theta_{c2} = 38.02°$, $l_2 = 0.0075$ m.
For crack 3, $\theta_{c3} = 30.03°$, $l_3 = 0.0066$ m.

The initial cracking state is as shown in Fig. 6(a).

According to Eqs. (22) and (23), the fracture toughness after the cracks expanding are as follows

As for crack 1, $K_{IC} = 0.4525$ Mpa·m$^{1/2}$, $K_{IIC} = 0.3622$ Mpa·m$^{1/2}$.
As for crack 2, $K_{IC} = 0.4875$ Mpa·m$^{1/2}$, $K_{IIC} = 0.3345$ Mpa·m$^{1/2}$.
As for crack 3, $K_{IC} = 0.5375$ Mpa·m$^{1/2}$, $K_{IIC} = 0.3685$ Mpa·m$^{1/2}$.

According to the Eqs. (14) and (21) and follow Eqs.

$$\theta_c = \arccos\frac{3K_{\mathrm{II}}^2 + \sqrt{K_{\mathrm{I}}^4 + 8K_{\mathrm{I}}^2 K_{\mathrm{II}}^2}}{K_{\mathrm{I}}^2 + 9K_{\mathrm{II}}^2} \tag{26}$$

$$\begin{aligned}&(3-4\mu-\cos\theta)(1+\cos\theta)K_I^2 + 4\sin\theta(2\mu-1+\cos\theta)K_I K_{II}\\&+[4(1-\mu)(1-\cos\theta)+(1+\cos\theta)(3\cos\theta-1)]K_{II}^2 = 4(1-2\mu)K_{Ic}^2\end{aligned} \tag{27}$$

The crack angle and expanding length of the first expanding are as follows,

As for crack 1, $\theta_{c1} = 56.45°$, $l_1 = 0.0011$ m.
As for crack 2, $\theta_{c2} = 48.22°$, $l_2 = 0.0014$ m.
As for crack 3, $\theta_{c3} = 55.26°$, $l_3 = 0.009$ m.

The first expanding state is as shown in Fig. 6(b).

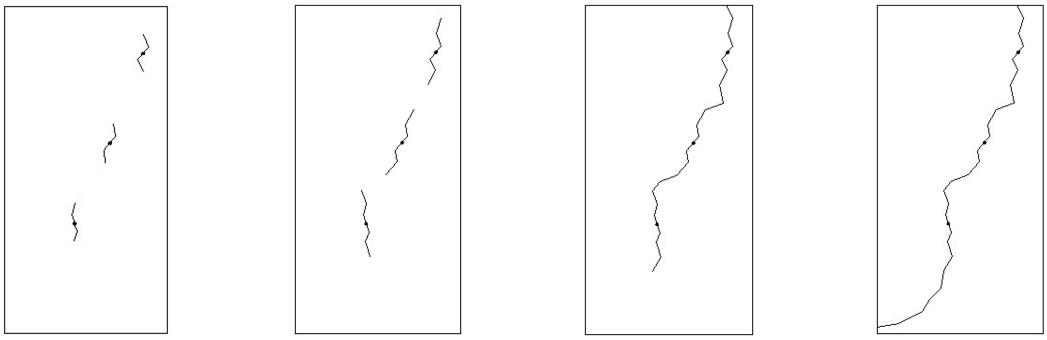

(a) Initial cracking state (b) First expanding (c) Second expanding (d) Communicating state

Fig. 6 Fracture process of sandstone specimen

Considering the interrelationship of cracks, the fracture toughness of three cracks are as follows,

As for crack 1, K_{IC} = 0.2624 Mpa·m$^{1/2}$, K_{IIC} = 0.2204 Mpa·m$^{1/2}$.
As for crack 2, K_{IC} = 0.3237 Mpa·m$^{1/2}$, K_{IIC} = 0.2854 Mpa·m$^{1/2}$.
As for crack 3, K_{IC} = 0.3375 Mpa·m$^{1/2}$, K_{IIC} = 0.2864 Mpa·m$^{1/2}$.

The crack angle and expanding length of the second expanding are as follows,

As for crack 1, θ_{c1} = 55.14°, l_1 = 0.014 m.
As for crack 2, θ_{c2} = 47.24°, l_2 = 0.012 m.
As for crack 3, θ_{c3} = 50.14°, l_3 = 0.011 m.

The second expanding state is as shown in Fig. 6(c).

Based on above analysis, when $K_I > K_{IC}$, the cracks will communicate, and the rock will be broken.

The communicating state is as shown in Fig. 6(d).

Comparison the fracture path in Figs. 6 and 5, it can be found that, the two fracture paths are coincided well.

For the limestone, the fracture toughness of crack modes I and II for three cracks at beginning are all K_{IC} = 0.52 Mpa·m$^{1/2}$ and K_{IIC} = 0.28 Mpa·m$^{1/2}$. The friction coefficient is 0.25.

Using the same analysis as that of the sandstone, the follow results can be obtained.

The initial cracking angles and initial cracking lengths of the cracks are as follows,

As for crack 1, θ_{c1} = 45.87°, l_1 = 0.017 m.
As for crack 2, θ_{c2} = 47.05°, l_2 = 0.012 m.
As for crack 3, θ_{c3} = 58.25°, l_3 = 0.011 m.

The crack angle and expanding length of the first expanding are as follows,

As for crack 1, θ_{c1} = 60.12°, l_1 = 0.018 m.
As for crack 2, θ_{c2} = 54.02°, l_2 = 0.015 m.
As for crack 3, θ_{c3} = 57.04°, l_3 = 0.015 m.

The crack angle and expanding length of the second expanding are as follows,

As for crack 1, θ_{c1} = 57.11°, l_1 = 0.020 m.
As for crack 2, θ_{c2} = 48.38°, l_2 = 0.017 m.

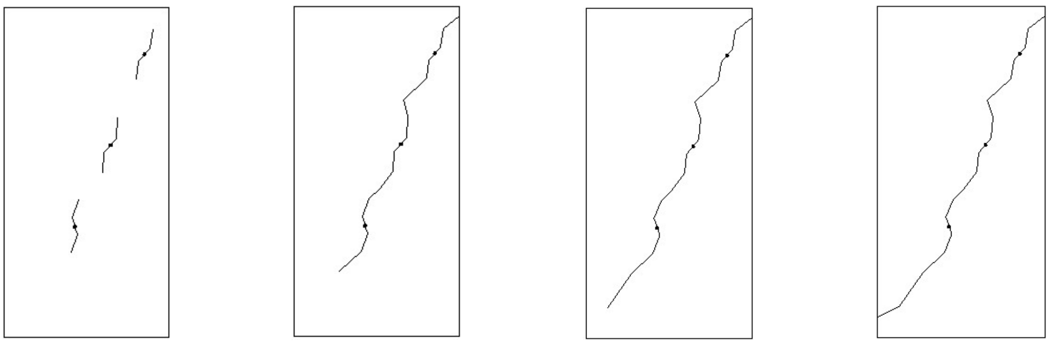
(a) Initial cracking state (b) First expanding (c) Second expanding (d) Communicating state

Fig. 7 Fracture process of limestone specimen

As for crack 3, θ_{c3} = 51.42°, l_3 = 0.019 m.

The fracture process is as shown in Fig. 7.

Comparison the fracture path in Figs. 7 and 5, it can also be found that, the two fracture paths by theory in this study and by experiment are coincided well.

Because the fracture path by the theory in this study is similar with the experimental one, the theory analysis in this study is feasible.

4. Conclusions

Considering the effect of the chemical erosion, fracture factor of rock is reduced. And the damage variable is applied to express the change of fracture stress. Then, the fracture criterion of rock under chemical erosion is constructed. Using this fracture criterion, the initial crack, crack expanding and crack communication can all be analyzed. And then, the fracture path of rock can be found. By one experiment of rock fracture under chemical erosion, the proposed fracture criterion is verified. From the initial crack, crack expanding and crack communication, the results of the theory are all agree with the experimental results well.

Acknowledgments

The financial supports from The Fundamental Research Funds for the Central Universities under Grant No. 2014B17814, 2014B07014 and B15020060 are gratefully acknowledged.

References

Chen, L., Duveau, G., Poutrel, A., Jia, Y., Shao, J.F. and Xie, N. (2014), "Numerical study of the interaction between adjacent galleries in a high-level radioactive waste repository", *Int. J. Rock Mech. Min.*, **71**, 405-417.

Ding, W.X. and Feng, X.T. (2009), "Damage effect and fracture criterion of rock with multi-preexisting cracks under chemical erosion", *Chin. J. Geotech. Eng.*, **31**(6), 899-904. [In Chinese]

Feng, X.T., Ding, W.X., Yao, H.Y. and Chen, S.L. (2010), *Coupled Chemical Stress Effect on Rock*

Fracturing Process, Science Press, Beijing, China. [In Chinese]
Gao, W., Wang, L. and Yang, D.Y. (2011), "Study on rock fracture failure criterion based on energy principles", *Adv. Sci. Lett.*, **4**(3), 869-874.
Gao, G., Yao, W., Xia, K. and Li, Z. (2015), "Investigation of the rate dependence of fracture propagation in rocks using digital image correlation (DIC) method", *Eng. Fract. Mech.*, **138**, 146-155.
Grgic, D. and Giraud, A. (2014), "The influence of different fluids on the static fatigue of a porous rock: Poro-mechanical coupling versus chemical effects", *Mech. Mater.*, **71**, 34-51.
Gross, D. and Seelig, T. (2011), *Fracture Mechanics with Introduction to Micromechanics*, Springer-Verlag, Berlin, Germany.
Guo, J.C., Liu, H.F., Zhu, Y.Q. and Liu, Y.X. (2014), "Effects of acid–rock reaction heat on fluid temperature profile in fracture during acid fracturing in carbonate reservoirs", *J. Petrol. Sci. Eng.*, **122**, 31-37.
Horri, H. and Nemat-Nasser, S. (1985), "Compression-induced microcrack growth in brittle solids: Axial splitting and shear failure", *J. Geophys. Res.*, **90**(B4), 3105-3125.
Jaeger, J.C., Cook, N.G.W. and Zimmerman, R. (2009), *Fundamentals of Rock Mechanics*, Wiley-Blackwell, Hoboken, NJ, USA.
Kazempour, M., Sundstrom, E. and Alvarado, V. (2012), "Geochemical modeling and experimental evaluation of high-pH floods: Impact of water-rock interactions in sandstone", *Fuel*, **92**(1), 216-230.
Li, F.B., Sheng, J.C., Zhan, M.L., Xu, L.M., Wu, Q. and Jia, C.L. (2014), "Evolution of limestone fracture permeability under coupled thermal, hydrological, mechanical, and chemical conditions", *J. Hydrodyn.*, *Ser. B*, **26**(2), 234-241.
Liu, T.Y., Cao, P. and Lin, H. (2014), "Damage and fracture evolution of hydraulic fracturing in compression-shear rock cracks", *Theor. Appl. Fract. Mec.*, **74**, 55-63.
Min, K.B., Rutqvist, J. and Elsworth, D. (2009), "Chemically and mechanically mediated influences on the transport and mechanical characteristics of rock fractures", *Int. J. Rock Mech. Min.*, **46**(1), 80-89.
Mukhopadhyay, S., Liu, H.H., Spycher, N. and Kennedy, B.M. (2013), "Impact of fluid–rock chemical interactions on tracer transport in fractured rocks", *J. Contam. Hydrol.*, **154**, 42-52.
Pandey, S.N., Chaudhuri, A., Kelkar, S., Sandeep, V.R. and Rajaram, H. (2014), "Investigation of permeability alteration of fractured limestone reservoir due to geothermal heat extraction using three-dimensional thermo-hydro-chemical (THC) model", *Geothermics*, **51**, 46-62.
Poulet, T., Karrech, A., Regenauer-Lieb, K., Fisher, L. and Schaubs, P. (2012), "Thermal–hydraulic–mechanical–chemical coupling with damage mechanics using ESCRIPTRT and ABAQUS", *Tectonophysics*, **526-529**, 124-132.
Pu, C.Z. and Cao, P. (2012), "Failure characteristics and its influencing factors of rock-like material with multi-fissures under uniaxial compression", *T. Nonferr. Metal. Soc.*, **22**(1), 185-191.
Taron, J., Elsworth, D. and Min, K.B. (2009), "Numerical simulation of thermal-hydrologic-mechanical-chemical processes in deformable, fractured porous media", *Int. J. Rock Mech. Min.*, **46**(5), 842-854.
Wang, Q., Zhou, Y.C., Wang, G., Jiang, H.W. and Liu, Y.S. (2012), "A fluid-solid-chemistry coupling model for shale wellbore stability", *Petrol. Explor. Dev.*, **39**(4), 508-513.
Wei, M.D., Dai, F., Xu, N.W., Xu, Y. and Xia, K. (2015), "Three-dimensional numerical evaluation of the progressive fracture mechanism of cracked chevron notched semi-circular bend rock specimens", *Eng. Fract. Mech.*, **134**, 286-303.
Yu, Q.L., Zhu, W.C., Tang, C.A. and Yang, T.H. (2014), "Impact of rock microstructures on failure processes-Numerical study based on DIP technique", *Geomech. Eng.*, *Int. J.*, **7**(4), 375-401.
Zhang, H.B., Zhang, W., Lv, L. and Feng, Y. (2010), "Effect of fissure water on mechanical characteristics of rock mass", *Min. Sci. Tech.*, **20**(6), 846-849.
Zhao, Z.H., Liu, L.C., Neretnieks, I. and Jing, L.R. (2014), "Solute transport in a single fracture with time-dependent aperture due to chemically medicated changes", *Int. J. Rock Mech. Min.*, **66**, 69-75.

CC